Published in final edited form as:
Dev Biol. 2014 September 1; 393(1): 124–136. doi:10.1016/j.ydbio.2014.06.013.

Loss of VHL in mesenchymal progenitors of the limb bud alters multiple steps of endochondral bone development

Laura Mangiavini[1,2,3,4,#], **Christophe Merceron**[1,2,5,6,#], **Elisa Araldi**[3], **Richa Khatri**[3], **Rita Gerard-O'Riley**[2], **Tremika LeShan Wilson**[1,2,3], **Erinn B. Rankin**[3,7], **Amato J. Giaccia**[7], and **Ernestina Schipani**[1,2,3,8,*]

[1]Department of Orthopaedic Surgery, Medical School, University of Michigan, Ann Arbor, MI 48109, USA

[2]Division of Endocrinology, Department of Medicine, School of Medicine, Indiana University, Indianapolis, IN 46202, USA

[3]Endocrine Unit, Massachusetts General Hospital-Harvard Medical School, Boston, MA 02114, USA

[4]Department of Orthopaedic and Traumatology, Milano-Bicocca University, 20900, Monza (MB), Italy

[5]Inserm, UMRS 791-LIOAD, Centre for Osteoarticular and Dental Tissue Engineering, Group STEP 'Skeletal Tissue Engineering and Physiopathology', 44042 Nantes, France

[6]LUNAM, Nantes University, Faculty of Dental Surgery, Nantes, France

[7]Division of Radiation and Cancer Biology, Department of Radiation Oncology, Stanford University, Stanford, CA 94303-5152, USA

[8]Division of Endocrinology, Department of Medicine, Medical School, University of Michigan, Ann Arbor, MI 48109, USA

Abstract

Adaptation to low oxygen tension (hypoxia) is a critical event during development. The transcription factors Hypoxia Inducible Factor-1α (HIF-1α) and HIF-2α are essential mediators of the homeostatic responses that allow hypoxic cells to survive and differentiate. Von Hippel Lindau protein (VHL) is the E3 ubiquitin ligase that targets HIFs to the proteasome for degradation in normoxia. We have previously demonstrated that the transcription factor HIF-1α is essential for survival and differentiation of growth plate chondrocytes, whereas HIF-2α is not necessary for fetal growth plate development. We have also shown that VHL is important for endochondral bone development, since loss of VHL in chondrocytes causes severe dwarfism. In this study, in

[*]***Corresponding Author***: Ernestina Schipani, University of Michigan, Medical School, A. Alfred Taubman Biomedical Science Research Bldg., 109 Zina Pitcher Place, Room 2007, Ann Arbor, MI 48109, Tel: +1-734-647-2274, eschipan@med.umich.edu.
[#]These authors have equally contributed to the study.

order to expand our understanding of the role of VHL in chondrogenesis, we conditionally deleted VHL in mesenchymal progenitors of the limb bud, i.e. in cells not yet committed to the chondrocyte lineage. Deficiency of VHL in limb bud mesenchyme does not alter the timely differentiation of mesenchymal cells into chondrocytes. However, it causes structural collapse of the cartilaginous growth plate as a result of impaired proliferation, delayed terminal differentiation, and ectopic death of chondrocytes. This phenotype is associated to delayed replacement of cartilage by bone. Notably, loss of HIF-2α fully rescues the late formation of the bone marrow cavity in VHL mutant mice, though it does not affect any other detectable abnormality of the VHL mutant growth plates. Our findings demonstrate that VHL regulates bone morphogenesis as its loss considerably alters size, shape and overall development of the skeletal elements.

Keywords

endochondral bone development; limb bud mesenchyme; von Hippel Lindau; Hypoxia Inducible Factor

INTRODUCTION

The ability of a cell to adapt to low oxygen tension (hypoxia) is critical both in pathological settings such as cancer and ischemia, and in normal development and differentiation [1].

The transcription factors Hypoxia Inducible Factor-1α (HIF-1α) and HIF-2α are crucial mediators of the homeostatic responses that allow hypoxic cells to survive and differentiate [2]. These proteins trigger a range of autonomous, autocrine, paracrine and endocrine effects with the overall goal of increasing oxygen delivery to tissues while decreasing their oxygen consumption, and thus promoting cell survival and differentiation [3–5].

HIF is a heterodimeric protein that results from the association between HIF-α and HIF-β subunits [6]. Three distinct forms of HIF-α and HIF-β do exist, and they are each the product of distinct paralogue genes [7, 8]. Each alpha subunit is able to bind any of the beta subunit to form a functional transcription factor. The beta subunit is constitutively expressed, whereas the alpha subunit is the oxygen-regulated element of the complex. In normoxia, a family of HIF prolyl-4-hydroxylases (PHDs) is responsible for the hydroxylation of two proline residues (P402 and P564) in the oxygen dependent degradation domain of HIF-1α [9, 10]. The E3 ubiquitin ligase von Hippel-Lindau (VHL) binds to the hydroxylated HIF-1α, and targets it to the proteasome for degradation [9, 11]. In hypoxia, hydroxylation of HIF-1α is inefficient, and thus HIF-1α migrates to the nucleus, binds HIF-1β, and hence promotes transcription of genes that have hypoxia responsive elements in their promoter region. The HIF-2α isoform is regulated by oxygen with a modality similar to HIF-1α [12].

The importance of VHL for proteolysis of HIF-1α and HIF-2α is highlighted by the finding that cells lacking functional VHL are unable to degrade these transcription factors, ultimately resulting in their accumulation [9, 11, 13, 14]. However, VHL has also a variety of biological activities including control of the cell cycle, regulation of matrix proteins,

interaction with the cytoskeleton and with the primary cilia that are HIF-independent [15, 16].

The fetal growth plate is a suitable model to study cellular adaptation to hypoxia during development [17]. Bone can form through two different mechanisms, intramembranous and endochondral. While the flat bones of the skull develop from mesenchymal cells that directly differentiate into osteoblasts (intramembranous bone formation), the other skeletal elements derive from a chondrocyte anlage that is replaced by bone [18–21]. This latter process is called endochondral bone development.

During endochondral bone development, mesenchymal cells first condense; cells within these condensations next differentiate into chondrocytes and generate the fetal growth plate. Growth plate chondrocytes are highly proliferative, and while they divide, they also pile up to form a columnar layer. The most distal cells of the columnar layer stop proliferating, exit the cell cycle, and differentiate into hypertrophic chondrocytes, which mineralize their surrounding matrix. The cartilaginous mold is then invaded by blood vessels and replaced by bone at two sites, the primary spongiosa and the secondary ossification center, respectively [19, 22, 23]. In parallel to the chondrocyte differentiation process, three-layered interzones that will give origin to the prospective synovial joints are specified; formation of the synovial space occurs upon cavitation of these interzones [24, 25]. Consistent with its avascularity, the murine fetal growth plate displays a gradient of oxygenation with an inner, hypoxic region [26].

The VHL/HIF pathway impacts numerous aspects of cartilage and bone biology. In particular, during growth plate development, HIF-1α is required for timely differentiation of mesenchymal cells into chondrocytes, for chondrocyte survival and for joint specification [26, 27]. Therefore, this transcription factor is necessary for endochondral bone development. Conversely, HIF-2α is virtually dispensable, as deficiency of HIF-2α causes only a modest and transient delay of chondrocyte terminal differentiation [28]. We have also recently reported an important role of VHL in endochondral bone development [29]. Mice lacking VHL in chondrocytes display a striking growth plate phenotype characterized by hypocellularity, impaired proliferation, and increased cell size in the round proliferative zone. These features eventually lead to severe dwarfism. Notably, loss of both VHL and HIF-1α in chondrocytes causes a growth plate phenotype identical to the one described in HIF-1α null animals [26]; HIF-1α is thus epistatic to VHL.

In order to better understand the role of VHL in the early steps of chondrogenesis, we genetically deleted VHL in mesenchymal progenitors of the limb bud, i.e. in cells that will give origin to the cartilage anlage by differentiating into chondrocytes but are not yet committed to the chondrocyte lineage. Our findings demonstrate that loss of VHL in limb bud mesenchyme alters multiple steps of endochondral bone development and, thus, they provide clear evidence that VHL is a crucial regulator of this process.

MATERIALS AND METHODS

All the experiments were performed using at least three independent biological replicates.

Generation of Mice

Generation and genotyping of the VHL (FVB/N), HIF-1α (FVB/N) and HIF-2α (C57/B6) floxed mice, PRX1-Cre (FVB/N), OSX-Cre (FVB/N) transgenic mice and ROSA26 mT/mG (FVB/N) reporter mice have been previously described [26, 30–33]. For all studies, *cre*-positive heterozygous floxed mice and *cre*-negative homozygous floxed mice, respectively, were used as controls. We found that the PRX1-Cre or OSX-Cre transgenes *per se* did not affect any of the phenotypes described in this manuscript. Generation of mT/mG mice has been previously described [34]. Of note, though in the same genetic background (FVB/N), in the study we strictly compared only mutant and control littermates. Moreover, at least three mutants and three controls were analyzed in each assay.

All procedures involving mice were performed in accordance with the NIH guidelines for use and care of live animals, and were approved by the Indiana University Institutional Animal Care and Use Committee (IACUC).

Growth curve, whole mount Alizarin Red S/Alcian Blue staining, routine histology, PAS staining, immunohistochemistry, in situ hybridization, TUNEL, Oil Red O staining, safranin-O staining and PCNA assay

Mice were weighed and measured at birth, p7, p14 and p21 to generate weight and growth curves, respectively. Whole mount Alizarin Red S/Alcian Blue staining was performed at birth as previously described [27]. For light microscopy, tissues from E10.5, E12.5, E13.5, E14.5, E15.5, E17.5 (delivered by caesarean section), newborn, p5, p17-p24 and 4 months were fixed in 4% Paraformaldehyde (PFA)/Phosphate Buffer Saline (PBS) (pH 7.4) for 48h at 4°C, and then stored in 70% ethanol at 4°C. Newborn and postnatal specimens were decalcified in 20% Ethylenediaminetetraacetic acid (EDTA) pH 7.5 at 4°C for up to 10 days. Paraffin blocks were prepared by standard histological procedures. Sections (5-6 mm thick) were cut from several levels of the block, and stained with Hematoxylin and Eosin.

For immunohistochemistry detection, paraffin sections from forelimbs of E10.5, E12.5, E13.5 and E15.5 mice embryos were treated with sodium citrate buffer pH 6 at 95°C for 10 minutes. Sections were then incubated with the following primary antibodies: VHL at 1:100 (BD 556347, BD Biosciences, San Jose, CA, USA), HIF-1α at a 1:100 (MAB1935, R&D Systems, Inc, Minneapolis, MN, USA) or HIF-2α at a 1:100 (NB100-122, Novus Biologicals, LLC, Littleton, CO, USA) overnight at 4°C. After incubation with the appropriate biotinylated secondary antibodies rabbit-anti-mouse (E 0413, Dako North America Inc., Carpinteria, CA, USA) or swine-anti-rabbit (E 0431, Dako North America Inc., Carpinteria, CA, USA), detection of the binding was carried out using the labeled streptavidin biotin (TSA) system following manufacturer's instructions (Perkin Elmer, Shelton CT, USA). Negative controls have been performed by omitting the primary antibody.

In situ hybridizations were performed on paraffin sections from hindlimbs and forelimbs of E13.5, E14.5, E15.5, p5 and p17 mice using complementary ^{35}S-labeled riboprobes, as previously described [27].

For PAS staining, paraffin sections from hindlimbs of newborn mice were stained using a PAS staining kit (Dako North America Inc., Carpinteria, CA, USA) according to the manufacturer's conditions.

TUNEL assay was performed on paraffin sections from hindlimbs of E15.5 and p17-p21 mice using an "*In situ* cell death detection" Kit (Roche Diagnostic, Mannheim, Germany). Sections were permeabilized with 0.1% TritonX100 in 0.1% sodium citrate; TUNEL assay was then carried on according to manufacturer's instructions.

Oil Red O staining was performed on liver fixed frozen sections at p17. Sections were incubated in 0.5% Oil Red O solution (Sigma Aldrich, St Louis, MO, USA) for 10 minutes, counterstained with Hematoxylin/Acetic water for 1 minute and coverslipped with aqueous mounting medium (Vector Laboratories, Burlingame, CA, USA).

For safranin-O staining, paraffin sections from forelimbs of E12.5, E13.5, E14.5 and E15.5 embryos were stained with safranin-O/fast green according to standard protocols [35].

PCNA assay was performed on paraffin sections from hindlimbs of p18 mice using the PCNA Invitrogen Kit (Invitrogen Corporation, Frederick, MD, USA), according to manufacturer's instructions.

BrdU Incorporation

E15.5 pregnant mice were injected intraperitoneally with 100 μg BrdU/12 μg FdU per gram body weight 2 hours prior to sacrifice. After sacrifice, embryo hindlimbs were dissected, fixed, and embedded in paraffin, and longitudinal sections across the tibia and femur were obtained. To identify actively proliferating cells, nuclei that had incorporated BrdU were detected using a Zymed BrdU immunostaining kit (Invitrogen Corporation, Frederick, MD, USA). Both total number of cells and BrdU-positive cells where manually counted in the Round Proliferative Layer (RPL) and in the Columnar Proliferative Layer (CPL) of the developing growth plates; proliferative rates were then calculated as number of BrdU-positive cells divided by total number of cells.

Cryosections

Hindlimbs, spines and livers were dissected from E15.5, p3 and p17 specimens, fixed in 4% PFA/PBS at 4°C for 48h and then stored in 70% ethanol at 4°C. Postnatal specimens were decalcified in 20% EDTA pH 7.5 at 4°C for up to 10 days. All the samples were subsequently placed in 30% Sucrose/PBS overnight and then embedded in optimum cutting temperature (OCT) embedding medium. Samples were sectioned at a thickness of 10 μm using a Leica cryostat. Sections were stored at −80°C for later use.

Image Acquisition

Images were acquired with Eclipse E800 (Nikon, Brighton, MI, USA). Additional images were captured with a Leica DM LB compound microscope (Leica Microsystems Inc., Buffalo Grove, IL, USA). For fluorescent images, frozen sections were dehydrated at RT overnight, rinsed in distilled water for 10 minutes and then overlayed with coverslips onto Vectashield Hard Set mounting medium with 4′,6-diamidino-2-phenylindole (DAPI)

(Vector Laboratories, Burlingame, CA, USA). Photos were taken using filters for Red Fluorescent Protein (RFP), fluorescein isothiocyanate (FITC) and DAPI.

Transmission Electron Microscopy (TEM) and Toluidine Blue staining

Growth plates were cleared completely of surrounding soft tissues, fixed in EM fixative (2.5% glutaraldehyde, 2.0% PFA, 0.025% calcium chloride in a 0.1 M sodium cacodylate buffer [pH 7.4]), and processed for EM. Two sets of consecutive sections were prepared: 1 μm sections stained with Toluidine Blue (5 minutes) to visualize the tissue morphology; 0.3 μm sections that were placed on top of grids for EM analysis. Samples were examined with a Phillips 301 transmission electron microscope and digital images were captured using an AMT (Advanced Microscopy Techniques) CCD camera at magnifications ranging from ×4500 to ×19,500.

X-Rays

Hindlimbs and forelimbs were analyzed by radiography, using an XPERT 80- L Cabinet X-ray System (Kevex-90Kv) (Kubtec X-Ray, Milford, CT, USA). Mice were imaged in a prone position at p21 using 2.7x magnification for CNTRL mice and 6.6x magnification for VHL, HIF1 and VHL-HIF1 mice. The images were acquired through Digicom NC software (Kubtec X-Ray, Milford, CT, USA).

Cell Isolation and Culture

Primary chondrocytes were isolated from newborn growth plates of VHL and CNTRL mice, respectively and cultured as described [36]. Deletion of *Vhlh* was confirmed by PCR analysis of the genomic DNA extracted from chondrocytes in culture, as previously reported [33].

Moreover, primary chondrocyte from newborn $VHL^{f/f}$ growth plates were also isolated for adenovirus infection [36]. On day 1 post-plating, adherent $VHL^{f/f}$ chondrocytes were infected with adenovirus containing either β-galactosidase or *cre*-recombinase (Vector Biolabs, Philadelphia, PA, USA) to generate wild-type chondrocytes or VHL null cells. All cells were incubated at 5% CO_2 under humidified atmosphere and media were changed every 2-3 days prior to collection.

Photos of cultured cells were taken with a Leica EC3 camera (Leica Microsystems Ltd, Switzerland).

dsDNA Quantification: PicoGreen Assay

Cells were rinsed twice with sterile, cold PBS (Cellgro, Mediatech, Inc, Manassas, VA, USA) prior to addition of 1 mL diluted lysis buffer, provided in Quant-iT PicoGreen dsDNA Assay kit (P7589, Life Technologies, Grand Island, NY, USA). Plates were wrapped in aluminum foil and placed at −80°C overnight at minimum. Plates were thawed at room temperature; samples were vigorously triturated individually and transferred to DNase-free microcentrifuge tubes. Samples and standards were loaded onto black 96-well plates. PicoGreen fluorescent nucleic acid stain (from kit) was added and plates were incubated at room temperature, protected from light, for 5 minutes. Sample fluorescence was measured

using the Synergy Mx microplate reader (BioTek, Winooski, VT, USA) with an excitation wavelength of ~480nm and emission wavelength of ~520nm.

Western Blotting

For protein extraction, cells were lysed in buffer containing sodium chloride, Tris, glycerol, Nonidet P-40 (Sigma Aldrich, St Louis, MO, USA), EDTA, and protease inhibitors (Roche Diagnostic, Mannheim, Germany). Bicinchoninic acid assay was performed for protein determination (Thermo Scientific, Rockford, Il, USA). Samples were analyzed by 10% SDS-PAGE gels (Bio-Rad Laboratories, Hercules, CA, USA) and subsequently transferred to Polyvinylidene fluoride (PVDF) membrane utilizing the BioRad Criterion system. Membranes were blocked in 5% milk in Tris-Buffered Saline with Tween 20 (TBST) and incubated in 5% milk with TBST at 4°C overnight with the following primary antibodies: HIF-1α (NB 100-479, Novus Biologicals, Littlelton, CO, USA) at 1:1000, HIF-2α (AF2997, R&D Systems, Inc., Minneapolis, MN, USA) at 1:200, BiP (3177S, Cell Signaling Technology, Inc., Danvers, MA, USA) at 1:1000 or p53 (VP-P952, Vector Laboratories, Inc., Burlingame, CA, USA) at 1:500. The membranes were then incubated with corresponding HRP-conjugated secondary antibodies donkey-anti-rabbit (Cell Signaling Technology, Inc., Danvers, MA, USA) or donkey-anti-goat (Santa Cruz Biotechnology, Inc., Santa Cruz, CA, USA) at 1:2000 for 1 hour in 5% milk with TBST. The blots were then incubated in Amersham ECL Plus Western Blotting System (GE Healthcare Biosciences, Pittsburgh, PA, USA), and chemiluminescent bands were visualized via the Image Quant LAS-4000 Fuji imaging system (Fujifilm Life Science, Tokyo, Japan). Quantification was performed using Image-J software (NIH). α-Tubulin antibody (Cell Signaling Technology, Inc., Danvers, MA, USA) was used to normalize protein amount.

Statistical Analysis

Histograms are represented as the mean of the replicates ± SD. Statistical differences were analyzed using the Student's t test. Differences with a p-value <0.05 were considered as statistically significant.

RESULTS

Generation of mice lacking VHL in mesenchymal progenitors of the limb bud

In order to define the role of VHL in the mesenchymal cells of the limb bud, we conditionally inactivated VHL in cells expressing *cre*-recombinase under the control of a PRX1 enhancer (PRX1-Cre). For this purpose, mice homozygous for the *Vhlh* conditional alleles (2-*loxP*) were crossed with PRX1-Cre mice to generate PRX1-Cre;$VHL^{f/f}$ mutant (VHL) mice and PRX1-Cre;$VHL^{f/+}$ or $VHL^{f/f}$ control (CNTRL) mice. Of note, PRX1-Cre;$VHL^{f/+}$ and $VHL^{f/f}$ mice were phenotypically identical, therefore for the purpose of this study they were used indistinctly.

PRX1-Cre mediates efficient *cre*-recombinase activity in mesenchymal progenitors that differentiate both into cartilage and bone, and into the soft tissue surrounding the cartilaginous primordia [32, 37]. The expression of PRX1-Cre in cartilage and in the surrounding soft tissues was confirmed using mT/mG reporter mice (mTmG) [34]. These

mice have *loxP* sites on either side of a membrane-targeted tandem dimer Tomato (mT) cassette, and express red fluorescence in all tissues. When bred to PRX1-Cre mice (PRX-mTmG), the mT cassette is deleted, allowing expression of the membrane-targeted EGFP (mG) cassette located downstream, in the tissues where *cre* is active. In E15.5 PRX-mTmG mice, both growth plate and surrounding soft tissues including the perichondrium displayed a positive EGFP signal, concomitant with the loss of the red fluorescent signal, indicating a high level of *cre* activity at these sites (Figure 1).

The VHL conditional allele contains 2-*loxP* sites flanking the *Vhlh* promoter and exon 1 [31]. Recombination of the VHL conditional allele in VHL chondrocytes was confirmed by genomic PCR analysis for the recombined (1-*loxP*) allele (Supplemental Figure 1, Panel A).

As predicted by the current model, an increased accumulation of both HIF-1α and HIF-2α proteins was observed by Western blot analysis of whole protein lysate extracted from VHL chondrocytes when compared to CNTRL (Supplemental Figure 1, Panel B). This accumulation was confirmed at the nuclear level by immunohistochemistry (IHC) on histological sections of E15.5 mutant and control growth plates (Supplemental Figure 1, Panel C).

Moreover, in agreement with these findings, expression of Vascular Endothelial Growth Factor (VEGF) mRNA, a classical downstream target of both HIF-1α and HIF-2α [38], was considerably augmented throughout the proliferative zone of the mutant growth plates when compared to CNTRL (Supplemental Figure 1, Panel D). VEGF is an important regulator of angiogenesis in endochondral bone development, and it is also a chondrocyte survival factor [39, 40]. Physiologically, VEGF mRNA is expressed both in hypertrophic chondrocytes, and, though at lower levels, in the inner portion of the proliferative zone, i.e. in the hypoxic region of the developing growth plate [39, 40].

Last, Transmission Electron Microscopy analysis and Toluidine blue staining of chondrocytes *in vivo* revealed the presence in the mutant cells of lipid droplets and glycogen accumulation, which are two hallmarks of VHL null specimens [41] (Supplemental Figure 1, Panel E: a and b, c and d). Periodic Acid Schiff (PAS) staining confirmed the accumulation of glycogen in mutant chondrocytes (Supplemental Figure 1, Panel F).

Taken together, these findings provide clear evidence that VHL was efficiently deleted and HIF-1α and HIF-2α were significantly stabilized in mutant growth plate chondrocytes.

Loss of VHL in mesenchymal progenitors of the limb bud generates shorter and developmentally delayed fetal bones by impairing proliferation of chondrocytes and by delaying their terminal differentiation

Mice with loss of VHL in limb bud mesenchyme were born with the expected mendelian frequency. Whole mount Alizarin Red S/Alcian Blue staining performed at birth showed that, whereas overall body size was similar (Figure 2: a and b), long bones were shorter, thinner and deformed in VHL mice in comparison to CNTRL (Figure 2: c-f), Of note, no obvious patterning defect was detectable in mutants (Figure 2: a and b).

The PRX1-Cre transgenic mouse expresses *cre*-recombinase at high level in the limb bud mesenchyme starting from E9.5, i.e. before mesenchymal condensations form [32]. Loss of HIF-1α in mesenchymal progenitors delays early chondrogenesis and joint development [27]. We thus asked the question whether loss of VHL affects these two processes.

IHC provided convincing evidence that VHL protein is expressed in wild type limb bud mesenchyme at E10.5, and that we had successfully knocked out VHL in mesenchymal cells at this early stage of development (Supplemental Figure 2, Panel A: a and b).

However, safranin-O staining of E12.5 forelimb autopods indicated that loss of VHL did not accelerate differentiation of mesenchymal progenitors into chondrocytes (Supplemental Figure 2, Panel B: a and b).

Consistent with this conclusion, at E13.5 both mutant and control chondrocytes in the autopod showed similar morphology, comparable glycosaminoglycans content (Supplemental Figure 2, Panel B: c and d), and equivalent levels of expression of Sox9 and type II collagen (Col2a1) mRNAs (Supplemental Figure 4, Panel C; a and b, c and d). Sox9 is the “master” transcription factor of chondrogenesis, and its mRNA is expressed in proliferative chondrocytes but not in hypertrophic cells [21]; Col2a1 mRNA is a classical chondrogenic marker.

Notably, loss of VHL did not affect the process of joint segmentation either, as suggested by the analysis of Growth Differentiation Factor 5 (GDF5) mRNA expression (Supplemental Figure 2, Panel C: e and f). GDF5 is one of the earliest markers of joint specification, and it can be detected before interzones become histologically evident [42, 43].

Differently from early chondrogenesis, the subsequent steps of endochondral bone development were severely altered by loss of VHL. In particular, E13.5 mutant stylopods were already considerably smaller than controls, as indicated by H&E staining and by Col2a1 mRNA expression (Figure 3, Panel A: a-d). Moreover, chondrocyte terminal differentiation was severely delayed in VHL specimens in comparison to CNTRL, as shown by the uninterrupted expression of Sox9 mRNA (Figure 3, Panel A: e and f), the smaller domain of type X collagen (Col10a1) mRNA (Figure 3, Panel A: g and h), and the lack of osteopontin (SPP1) mRNA (Figure 3, Panel A: i and j). Col10a1 is a classical marker of hypertrophic chondrocytes, and its mRNA is already detectable immediately before hypertrophy occurs; it is then down regulated in the late hypertrophic chondrocytes located at the border with the primary spongiosa [21]. SPP1 mRNA is produced by late hypertrophic cells [21].

In addition, data collected by routine histology (Supplemental Figure 3: a and b) and by *in situ* hybridization analysis of E14.5 stylopods, namely persistence of Col2a1 mRNA in the center of the cartilaginous element and presence of one single domain of Col10a1 mRNA in mutant elements (Supplemental Figure 3: c and d, e and f), further supported the notion that at this developmental stage mutant hypertrophic chondrocytes, differently from controls, had not yet transitioned into late hypertrophic cells, which do not express Col2a1 mRNA and display lower amounts of Col10a1 mRNA.

Last, consistent with the hypothesis that loss of VHL delays endochondral bone development, formation of the bone marrow cavity was delayed in mutant specimens in comparison to controls (Figure 3, Panel B: a and b), as confirmed by the larger domains of Col2a1 and Col10a1 mRNA expression in E15.5 mutant stylopods (Figure 3, Panel B: c and d, e and f), and by the persistence in mutants of a safranin-O positive matrix in a region that was already occupied by bone marrow in control specimens (Figure 3, Panel B: g and h).

In line with our previous findings obtained in mutant mice in which VHL had been deleted in cells already committed to the chondrocyte lineage [29], a significant impairment of chondrocyte proliferation in both round proliferative and columnar layers was also detected in mutant fetal growth plates, as indicated by BrdU analysis (Figure 4, Panel A). Moreover, as previously reported [29], mutant chondrocytes in the round proliferating zone of the fetal growth plate were abnormally enlarged with a higher cytoplasm to nucleus ratio (Figure 4, Panel B).

In addition to their shortening, loss of VHL in limb bud mesenchyme caused deformities of the forelimb zeugopod as shown by H&E (Figure 5, Panel A: a and c), and by *in situ* hybridization analysis for Col2a1 and Col10a1 mRNAs (Figure 5, Panel A: b, d and e) of 15.5 specimens. Of note, these deformities, which were still detectable postnatally by X-Rays (Figure 5, Panel B), affected the same bone at the same location, consistently displayed the same shape, and had full penetrance and expressivity (data not shown).

Collectively, our findings demonstrate that loss of VHL in limb bud mesenchyme does not alter either chondrogenic differentiation of mesenchymal progenitors or joint development, but it impairs proliferation of chondrocytes, delays their terminal differentiation and results in bone deformities at specific sites.

Loss of VHL in mesenchymal progenitors of the limb bud causes massive chondrocyte death associated to complete growth arrest and lack of the secondary ossification center in the postnatal growth plate

After birth, mutant mice became overall smaller than control littermates (Figure 6, Panel A and B: a); they lost weight (Figure 6, Panel B: b), and eventually died at 4 weeks of age for a cause yet to be identified.

Notably, at postnatal time points, loss of VHL blocked the formation of the secondary ossification center, and led to the complete disappearance of both the columnar and the hypertrophic layers (Figure 7, a-d). This phenotype was likely the result of the severe impairment of proliferation and the profound delay of terminal differentiation observed at earlier time points. Curiously, islets of hypertrophic cartilage persisted within the bone marrow (Figure 7, b and d), which suggests that a very disorganized cartilage-to-bone transition occurred in VHL mutants.

Interestingly, Col2a1 mRNA expression was dramatically down regulated in the round proliferative chondrocyte layer of the postnatal growth plate (Figure 7: e and f). This somehow unusual finding was not due to either chondrocyte hypertrophy or to chondrocyte transdifferentiation into fibroblasts, as mutant chondrocytes did not express either Col10a1

mRNA (data not shown) or type I collagen (Col1a1) mRNA (Figure 7: g and h), respectively, but it was most likely the consequence of massive cell death (Figure 7: i and j). Cell death was associated to complete arrest of cell proliferation, as indicated by PCNA staining (Figure 7: k and l). Curiously, no sign of chondrocyte death had been detected at prenatal time points (data not shown).

Postnatal VHL mutants also displayed a smaller axial skeleton (Figure 6, Panel A) and, histologically, a very modest delay of replacement of cartilage by bone in the vertebral bodies, though their overall architecture was normal (Supplemental Figure 4, Panel A). This quite mild phenotype was not due to ectopic expression of the *cre* in the axial skeleton, as shown by the use of the mTmG reporter (Supplemental Figure 4, Panel B). The lack of ectopic expression of *cre* in the vertebral bodies is consistent with the observation that, differently from the postnatal time points, the overall size of the axial skeleton of VHL mutants at birth was normal, as shown by whole mount Alizarin Red S/Alcian Blue staining (Figure 2: a and b). Thus, the postnatal axial skeleton phenotype of VHL mutants was most likely contributed by systemic factors.

Along these lines, mutant mice displayed a liver phenotype characterized by the presence of hemorrhagic cysts (Supplemental Figure 5, Panel A: a-c), angiectases, and abnormal proliferation of fibroblastoid cells, which were initially located in close proximity to blood vessels, but eventually invaded and replaced the liver parenchyma (Supplemental Figure 5, Panel A: d-g). Moreover, consistent with the deletion of VHL, we observed a unique accumulation of lipids in the mutant hepatocytes by Oil Red O staining (Supplemental Figure 5, Panel A: h and i). All in all, these lesions were reminiscent of the hemangioblastomas that develop in liver upon specific deletion of VHL in hepatocytes [31]. Tissue surveys of the PRX-mTmG mice revealed ectopic activity of *cre*-recombinase in hepatocytes (Supplemental Figure 5, Panel B), which, to our knowledge, has not previously been reported.

Importantly, this liver phenotype was not present at birth (Supplemental Figure 5, Panel C), but it developed postnatally and could explain, at least in part, the overall decrease of body size and the premature death of VHL mutants.

Taken together, our data indicate that the dramatic decrease of body size and weight of VHL mutant mice postnatally is most likely the consequence of systemic factors including a potential liver failure. However, and most importantly, the postnatal limb phenotype of VHL mice appears to be very specific and not contributed by systemic factors for two main reasons: first, differently from the long bones, the postnatal vertebral bodies in VHL mutants are histologically very similar to controls, except for an extremely mild delay of replacement of cartilage by bone; second, no limb abnormalities have been reported upon specific deletion of VHL in hepatocytes [31].

Loss of VHL in mesenchymal progenitors of the limb bud results in a severe bone phenotype, which, however, does not significantly contribute to the growth plate abnormalities

Since the PRX1-Cre transgene is expressed in the osteochondroprogenitors that give origin not only to cartilage but also to bone [32, 37], to be thorough we attempted to study trabecular bone in mutant and control tibias around p21 by routine histology, despite the premature death of the mutant mice. This analysis revealed a dramatic increase of trabecular bone in mutant specimens as shown by X-rays and routine histology (Figure 8). This excessive trabecularization was associated to dilated bone marrow blood vessels and to the presence of a stromal cell population in between the bony trabeculae with only a few islets of hematopoietic cells (Figure 8, Panel B: b). The premature demise of the VHL mutant mice around p28 precluded us from pursuing a further and extensive characterization of their bone phenotype. Nonetheless, the finding confirmed our previous data obtained in mutant mice in which we had specifically deleted VHL in cells of the osteoblast lineage at different stages of differentiation [33, 44].

We next asked whether the postnatal growth plate abnormalities observed in VHL mutant mice, and in particular the disorganized transition from cartilage to bone, was somehow the consequence of their bone phenotype. To specifically address this question, we conditionally knocked out VHL in cells of the osteoblast lineage using OSTERIX-Cre transgenic mice (OSX-Cre) [45]; we thus generated mutants (OSX-VHL$^{f/f}$), *cre*-positive heterozygous floxed (OSX-VHL$^{f/+}$) and *cre*-negative homozygous floxed (VHL$^{f/f}$) controls. We then analyzed the developing growth plate at multiple time points from E15.5 to 4 months of age in all experimental groups.

As expected, mutant mice lacking VHL in cells of the osteoblast lineage dysplayed a dramatic accumulation of trabecular bone; conversely, their growth plate phenotype was extremely modest and mainly characterized by a quite mild and very transient delay of terminal differentiation (Supplemental Figure 6), which is consistent with the notion that in OSX-Cre transgenic mice, *cre* is also expressed in hypertrophic chondrocytes, though at a low level [46].

In light of these findings, we can thus conclude that mutant mice lacking VHL in limb bud mesenchyme exhibit, as expected, a dramatic bone phenotype, which most likely is not the cause of their severe growth plate abnormalities.

Of note, since in the PRX1-Cre transgenic mouse, *cre* is not active in the endothelium [32, 47], it is highly unlikely that any of the histological features dysplayed by the VHL mutant mice in either cartilage or bone is a consequence of deletion of VHL in endothelial cells.

Loss of HIF-2α in VHL deficient mesenchymal progenitors of the limb bud accelerates the replacement of cartilage by bone

In order to identify a possible role for HIF-1α in mediating at least in part the dramatic growth plate phenotype secondary to loss of VHL, we generated mice lacking both VHL and HIF-1α (VHL-HIF1) in limb bud mesenchyme. Notably, these double mutant mice had a dramatically abnormal postnatal growth plate that was virtually indistinguishable from the

mutant growth plate of mice lacking exclusively HIF-1α (Supplemental Figure 7). This finding shows that HIF-1α is indeed epistatic to VHL, and it thus confirmed what we had previously documented in a mutant model in which both proteins had been conditionally deleted by using a *cre*-recombinase driven by a fragment of the Col2a1 promoter [29].

Since also HIF-2α is stabilized in VHL mutant chondrocytes (Supplemental Figure 1, Panel B: a and c) we decided to study a possible role of this transcription factor in mediating some of the effects secondary to loss of VHL in limb bud mesenchyme. For this purpose, we generated mice lacking both VHL and HIF-2α in limb bud mesenchyme (VHL-HIF2). Mice were born with the expected mendelian frequency and they were viable, but they also died around p28 (data not shown).

Loss of HIF-2α did not correct the delayed hypertrophic differentiation observed in the VHL mutant growth plate, as indicated by routine histology and by *in situ* hybridization analysis for Col10a1 mRNA expression (Figure 9, Panel A: a and b, c and d). In addition, mice lacking both VHL and HIF-2α still displayed impaired chondrocyte proliferation, and massive postnatal cell death (Figure 9, Panel B and data not shown). Moreover, they had no histological evidence of formation of the secondary ossification center (data not shown).

However, loss of HIF-2α rescued the timely formation of the bone marrow cavity (Figure 9, Panel C) and accelerated the replacement of cartilage by bone with, consequently, complete disappearance of the hypertrophic layer at an even earlier time point than in VHL single mutants, as indicated by routine histology and by *in situ* hybridization analysis for Col10a1 mRNA expression (Figure 9, Panel D: a,c,e,g and b,d,f,h). This finding, which was somehow unexpected as loss of HIF-2α in limb bud mesenchyme determines only a modest and transient delay in chondrocyte terminal differentiation [28], suggests that HIF-2α may indeed have a fine tuning role at the interface between cartilage and bone.

Loss of VHL impairs proliferation and increases accumulation of BiP protein in chondrocytes *in vitro*

In order to start dissecting out the complex *in vivo* phenotype of mutant growth plate lacking VHL, we performed a series of *in vitro* analysis. For this purpose, we isolated chondrocytes from $VHL^{f/f}$ newborn mice as described in Materials and Methods. We next infected them with either β-galactosidase or *cre*-recombinase adenoviral constructs in order to obtain wild type (β-gal) and VHL null (cre) chondrocytes, respectively.

Cell density was considerably decreased in VHL null chondrocyte cultures; in addition, morphology of mutant cells appeared to be substantially different from controls, as VHL null chondrocytes had lost the classical “cobblestone” appearance and had rather assumed an elongated, fibroblastoid shape (Figure 10, Panel A). Analysis of DNA accumulation by Picogreen assay confirmed that loss of VHL had significantly impaired chondrocyte proliferation *in vitro* (Figure 10, Panel B) [48].

An extensive literature has suggested a complex relationship between the tumor suppressor gene p53 and VHL, which is often context-dependent [49–51]. Since the growth arrest observed in VHL mutant chondrocytes could in principle be mediated by stabilization of p53

in these cells, we analyzed accumulation of p53 protein in whole cell lysate of newborn chondrocytes isolated from mutant and control growth plate chondrocytes. Interestingly, p53 protein was not detectable in control chondrocytes, as also previously reported by others [52] and, more importantly, its expression was not up regulated in mutant chondrocytes (data not shown).

It has been reported that endoplasmic reticulum (ER) stress halts chondrocyte proliferation and differentiation and causes their death [50, 53–55]; moreover, VHL has been recently localized in the ER [16, 56]. We thus asked the question whether loss of VHL activates the unfolded protein response (UPR) in chondrocytes *in vitro*. For this purpose, we analyzed expression of the Binding immuglobulin Protein (BiP or GRP78), which is a marker of UPR [57]. Notably, levels of BiP expression were significantly higher in VHL null chondrocytes when compared to controls (Figure 10, Panel C), which suggests that ER stress could be one of the pathogenetic events involved in the generation of the complex growth plate phenotype caused by loss of VHL in mesenchymal progenitors.

DISCUSSION

In this study, we report the first conditional knockout of VHL in mesenchymal progenitors of the limb bud, i.e. in cells not yet committed to the chondrocyte lineage. Deficiency of VHL in limb bud mesenchyme does not alter the timely differentiation of mesenchymal cells into chondrocytes. However, it causes structural collapse of the cartilaginous growth plate as a result of impaired proliferation, delayed terminal differentiation and ectopic death of chondrocytes. This phenotype is associated to delayed replacement of cartilage by bone. Loss of HIF-2α fully rescues the late formation of the bone marrow cavity in VHL mutant mice, though it does not affect any other detectable abnormality of the VHL mutant growth plates. Our findings demonstrate that VHL regulates bone morphogenesis as its loss considerably alters size, shape and overall development of the skeletal elements.

Interestingly, the growth plate phenotype of mutant mice lacking VHL in limb bud mesenchyme is definitively more severe than the one we reported upon deletion of VHL in already differentiated chondrocytes [29]. Moreover, our novel mouse model displays unique features, including a dramatic delay of hypertrophy as well as a massive postnatal chondrocyte death. We do not exactly know why the two mutant mice differ from each other, but it is tempting to speculate that both the diverse spatial and temporal distribution of the *cre*-recombinase and the potential differences in the efficiency of deletion of the floxed allele are factors that could contribute to generate the phenotypic differences we detected between the two mutant lines.

The analysis of VHL mutant bones also revealed a series of intriguing paradoxes. In particular, a delay of terminal differentiation similar to the one observed in VHL deficient mice has also been described in mice lacking HIF-1α either in limb bud mesenchyme [27] or in chondrocytes [26, 40]. This apparent resemblance, however, is most likely the result of profoundly different molecular and/or cellular mechanisms. Along these lines, it is important to note that loss of HIF-1α in limb bud mesenchyme delays differentiation of mesenchymal progenitors into chondrocytes, and, thus, it is highly probable that this initial delay of early

chondrogenesis contributes to slow down hypertrophy. Conversely, VHL does not affect the initial steps of chondrogenesis. In addition, loss of HIF-1α in both limb bud mesenchyme and in chondrocytes causes a massive cell death phenotype in the fetal growth plate that is not initially present in the VHL mutants.

Though we yet do not know why chondrocytes lacking VHL display a significant delay of hypertrophy, however, in this study we provide evidence that this phenotype is not due to stabilization of HIF-2α, since it is not corrected by HIF-2α deletion.

The impairment of chondrocyte proliferation and the growth arrest we observed in VHL mutants is also paradoxical and surprising since VHL is a tumor suppressor gene, but it is well in agreement with previous findings by us and others [29, 58–60]. In addition, it is consistent with the notion that HIF-1α stabilization slows down cell proliferation [12], probably as part of a complex homeostatic response whose ultimate goal is likely to keep oxygen consumption in check. Interestingly, however, VHL has been reported to inhibit progression through the cell cycle in a HIF-1α-independent fashion [58]. It is thus possible that the decreased proliferation first and the virtual growth arrest later observed in VHL mutant growth plates could be the result of either HIF-1α-dependent or HIF-1α-independent VHL functions.

Loss of VHL, delays blood vessel invasion and the formation of both the primary and secondary ossification centers. This is another paradoxical finding since vascularization of the cartilage template, which is a required step in endochondral bone development, depends largely on VEGF, i.e. a classical downstream target of the HIF signaling pathway [38]. The delayed blood vessel invasion is, however, consistent with the overall delay of chondrocyte hypertrophy observed in VHL mutant bones. Moreover, it further highlights the intrinsic resistance of quiescent or proliferative cartilage to be invaded by blood vessels, despite increased expression of VEGF [29, 61].

Along the line of paradoxical findings, postnatal VHL chondrocytes display a severe cell death phenotype despite the stabilization of HIF-1α, which is a survival factor in the developing growth plate.

Lastly, loss of HIF-2α in the context of VHL mutant mice dramatically accelerates the replacement of cartilage by bone, but loss of HIF-2α in limb bud mesenchyme causes a transient and modest delay in hypertrophy mainly due to an impairment of differentiation of hypertrophic chondrocytes into late hypertrophic cells [28].

To this end, we do not have a full understanding of these paradoxes; however, our *in vitro* findings suggest that ER stress may be a contributing factor to the complex phenotype of VHL mutant growth plates. Along these lines, it has been shown that ER stress is an important pathogenetic event in some chondrodysplasias [50, 54, 55]. Moreover, the VHL protein has been associated to the ER [16, 56]. In our study, we report, for the first time to our knowledge, that deletion of VHL leads, with yet unknown mechanisms, to accumulation of BiP, a classical marker of UPR.

Of note, it has been recently reported that VHL regulates Sox9 expression in pancreas [62]. Moreover it is also known that ectopic expression of Sox9 in growth plate causes delayed terminal differentiation and cartilage vascularization associated with reduced bone growth [63, 64]. Therefore, a role of Sox9 in mediating some of the abnormal features we observe in VHL mutant growth plates cannot be excluded at this stage of investigation.

In conclusion, we demonstrated that VHL plays an important role in chondrocyte differentiation and survival; further studies will be necessary to unveil the detailed molecular mechanisms that lead to the severe abnormalities of endochondral bone development observed in mutant mice lacking VHL in mesenchymal progenitors of the limb bud.

Supplementary Material

Refer to Web version on PubMed Central for supplementary material.

ACKNOWLEDGMENTS

We thank Martin K. Selig for outstanding technical assistance with TEM.

We thank Drs. M. Celeste Simon, Randall S. Johnson and Volker H. Haase for providing HIF-2α$^{f/f}$, HIF-1α$^{f/f}$ and VHL$^{f/f}$ mice, respectively. We are very grateful to Dr. Karin Eisenger for precious advice about Western blot detection of HIF-2α.

We thank the Microscopy and Image-analysis Lab (MIL) at University of Michigan for providing us with outstanding instrumentation.

This work was supported by the NIH RO1 (AR065403-01) grant (to ES and AJG). Christophe Merceron received funding from the People Programme (Marie Curie Actions) of the European Union's Seventh Framework Programme (FP7/2007-2013) registered under the Research Executive Agency grant agreement n^{o}300388.

REFERENCES

1. Maes C, Carmeliet G, Schipani E. Hypoxia-driven pathways in bone development, regeneration and disease. Nat Rev Rheumatol. 2012; 8(6):358–366. [PubMed: 22450551]
2. Dunwoodie SL. The role of hypoxia in development of the Mammalian embryo. Dev Cell. 2009; 17(6):755–773. [PubMed: 20059947]
3. Rankin EB, Giaccia AJ. The role of hypoxia-inducible factors in tumorigenesis. Cell Death Differ. 2008; 15(4):678–685. [PubMed: 18259193]
4. Semenza GL. Regulation of cancer cell metabolism by hypoxia-inducible factor-11. Semin Cancer Biol. 2009; 19(1):12–16. [PubMed: 19114105]
5. Semenza GL. Hypoxia-inducible factors in physiology and medicine. Cell. 2012; 148(3):399–408. [PubMed: 22304911]
6. Wang GL, Jiang BH, Rue EA, Semenza GL. Hypoxia-inducible factor 1 is a basic-helix-loop-helix-PAS heterodimer regulated by cellular O2 tension. Proc Natl Acad Sci U S A. 1995; 92(12):5510–5514. [PubMed: 7539918]
7. Hirose K, Morita M, Ema M, Mimura J, Hamada H, Fujii H, Saijo Y, Gotoh O, Sogawa K, Fujii-Kuriyama Y. cDNA cloning and tissue-specific expression of a novel basic helix-loop-helix/PAS factor (Arnt2) with close sequence similarity to the aryl hydrocarbon receptor nuclear translocator (Arnt). Mol Cell Biol. 1996; 16(4):1706–1713. [PubMed: 8657146]
8. Takahata S, Sogawa K, Kobayashi A, Ema M, Mimura J, Ozaki N, Fujii-Kuriyama Y. Transcriptionally active heterodimer formation of an Arnt-like PAS protein, Arnt3, with HIF-1a, HLF, and clock. Biochem Biophys Res Commun. 1998; 248(3):789–794. [PubMed: 9704006]

9. Ivan M, Kondo K, Yang H, Kim W, Valiando J, Ohh M, Salic A, Asara JM, Lane WS, Kaelin WG Jr. HIFalpha targeted for VHL-mediated destruction by proline hydroxylation: implications for O2 sensing. Science. 2001; 292(5516):464–468. [PubMed: 11292862]
10. Jaakkola P, Mole DR, Tian YM, Wilson MI, Gielbert J, Gaskell SJ, von Kriegsheim A, Hebestreit HF, Mukherji M, Schofield CJ, Maxwell PH, Pugh CW, Ratcliffe PJ. Targeting of HIF-alpha to the von Hippel-Lindau ubiquitylation complex by O2-regulated prolyl hydroxylation. Science. 2001; 292(5516):468–472. [PubMed: 11292861]
11. Maxwell PH, Wiesener MS, Chang GW, Clifford SC, Vaux EC, Cockman ME, Wykoff CC, Pugh CW, Maher ER, Ratcliffe PJ. The tumour suppressor protein VHL targets hypoxia-inducible factors for oxygen-dependent proteolysis. Nature. 1999; 399(6733):271–275. [PubMed: 10353251]
12. Keith B, Johnson RS, Simon MC. HIF1alpha and HIF2alpha: sibling rivalry in hypoxic tumour growth and progression. Nat Rev Cancer. 2011; 12(1):9–22. [PubMed: 22169972]
13. Haase VH. The VHL tumor suppressor in development and disease: functional studies in mice by conditional gene targeting. Semin Cell Dev Biol. 2005; 16(4–5):564–574. [PubMed: 15908240]
14. Kamura T, Sato S, Iwai K, Czyzyk-Krzeska M, Conaway RC, Conaway JW. Activation of HIF1alpha ubiquitination by a reconstituted von Hippel- Lindau (VHL) tumor suppressor complex. Proc Natl Acad Sci U S A. 2000; 97(19):10430–10435. [PubMed: 10973499]
15. Hsu T. Complex cellular functions of the von Hippel-Lindau tumor suppressor gene: insights from model organisms. Oncogene. 2012; 31(18):2247–2257. [PubMed: 21996733]
16. Kaelin WG Jr. The von Hippel-Lindau tumour suppressor protein: O2 sensing and cancer. Nat Rev Cancer. 2008; 8(11):865–873. [PubMed: 18923434]
17. Provot S, Schipani E. Fetal growth plate: a developmental model of cellular adaptation to hypoxia. Ann N Y Acad Sci. 2007; 1117:26–39. [PubMed: 18056035]
18. Karsenty G. The complexities of skeletal biology. Nature. 2003; 423(6937):316–318. [PubMed: 12748648]
19. Kronenberg HM. Developmental regulation of the growth plate. Nature. 2003; 423(6937):332–336. [PubMed: 12748651]
20. Lefebvre V, Smits P. Transcriptional control of chondrocyte fate and differentiation. Birth Defects Res C Embryo Today. 2005; 75(3):200–212. [PubMed: 16187326]
21. Provot S, Schipani E. Molecular mechanisms of endochondral bone development. Biochem Biophys Res Commun. 2005; 328(3):658–665. [PubMed: 15694399]
22. Gerber HP, Vu TH, Ryan AM, Kowalski J, Werb Z, Ferrara N. VEGF couples hypertrophic cartilage remodeling, ossification and angiogenesis during endochondral bone formation. Nat Med. 1999; 5(6):623–628. [PubMed: 10371499]
23. Zelzer E, Olsen BR. Multiple roles of vascular endothelial growth factor (VEGF) in skeletal development, growth, and repair. Curr Top Dev Biol. 2005; 65:169–187. [PubMed: 15642383]
24. Khan IM, Redman SN, Williams R, Dowthwaite GP, Oldfield SF, Archer CW. The development of synovial joints. Curr Top Dev Biol. 2007; 79:1–36. [PubMed: 17498545]
25. Craig FM, Bentley G, Archer CW. The spatial and temporal pattern of collagens I and II and keratan sulphate in the developing chick metatarsophalangeal joint. Development. 1987; 99(3): 383–391. [PubMed: 2958266]
26. Schipani E, Ryan HE, Didrickson S, Kobayashi T, Knight M, Johnson RS. Hypoxia in cartilage: HIF-1alpha is essential for chondrocyte growth arrest and survival. Genes Dev. 2001; 15(21): 2865–2876. [PubMed: 11691837]
27. Provot S, Zinyk D, Gunes Y, Kathri R, Le Q, Kronenberg HM, Johnson RS, Longaker MT, Giaccia AJ, Schipani E. Hif-1alpha regulates differentiation of limb bud mesenchyme and joint development. J Cell Biol. 2007; 177(3):451–464. [PubMed: 17470636]
28. Araldi E, Khatri R, Giaccia AJ, Simon MC, Schipani E. Lack of HIF-2alpha in limb bud mesenchyme causes a modest and transient delay of endochondral bone development. Nat Med. 2011; 17(1):25–26. author reply 27-9. [PubMed: 21217667]
29. Pfander D, Kobayashi T, Knight MC, Zelzer E, Chan DA, Olsen BR, Giaccia AJ, Johnson RS, Haase VH, Schipani E. Deletion of Vhlh in chondrocytes reduces cell proliferation and increases

matrix deposition during growth plate development. Development. 2004; 131(10):2497–2508. [PubMed: 15128677]

30. Gruber M, Hu CJ, Johnson RS, Brown EJ, Keith B, Simon MC. Acute postnatal ablation of Hif-2alpha results in anemia. Proc Natl Acad Sci U S A. 2007; 104(7):2301–2306. [PubMed: 17284606]
31. Haase VH, Glickman JN, Socolovsky M, Jaenisch R. Vascular tumors in livers with targeted inactivation of the von Hippel-Lindau tumor suppressor. Proc Natl Acad Sci U S A. 2001; 98(4): 1583–1588. [PubMed: 11171994]
32. Logan M, Martin JF, Nagy A, Lobe C, Olson EN, Tabin CJ. Expression of Cre Recombinase in the developing mouse limb bud driven by a Prxl enhancer. Genesis. 2002; 33(2):77–80. [PubMed: 12112875]
33. Rankin EB, Wu C, Khatri R, Wilson TL, Andersen R, Araldi E, Rankin AL, Yuan J, Kuo CJ, Schipani E, Giaccia AJ. The HIF signaling pathway in osteoblasts directly modulates erythropoiesis through the production of EPO. Cell. 2012; 149(1):63–74. [PubMed: 22464323]
34. Muzumdar MD, Tasic B, Miyamichi K, Li L, Luo L. A global double-fluorescent Cre reporter mouse. Genesis. 2007; 45(9):593–605. [PubMed: 17868096]
35. Ivkovic S, Yoon BS, Popoff SN, Safadi FF, Libuda DE, Stephenson RC, Daluiski A, Lyons KM. Connective tissue growth factor coordinates chondrogenesis and angiogenesis during skeletal development. Development. 2003; 130(12):2779–2791. [PubMed: 12736220]
36. Aro E, Khatri R, Gerard-O'Riley R, Mangiavini L, Myllyharju J, Schipani E. Hypoxia-inducible factor-1 (HIF-1) but not HIF-2 is essential for hypoxic induction of collagen prolyl 4-hydroxylases in primary newborn mouse epiphyseal growth plate chondrocytes. J Biol Chem. 2012; 287(44): 37134–37144. [PubMed: 22930750]
37. Hilton MJ, Tu X, Wu X, Bai S, Zhao H, Kobayashi T, Kronenberg HM, Teitelbaum SL, Ross FP, Kopan R, Long F. Notch signaling maintains bone marrow mesenchymal progenitors by suppressing osteoblast differentiation. Nat Med. 2008; 14(3):306–314. [PubMed: 18297083]
38. Maes C, Araldi E, Haigh K, Khatri R, Van Looveren R, Giaccia AJ, Haigh JJ, Carmeliet G, Schipani E. VEGF-independent cell-autonomous functions of HIF-1alpha regulating oxygen consumption in fetal cartilage are critical for chondrocyte survival. J Bone Miner Res. 2012; 27(3): 596–609. [PubMed: 22162090]
39. Maes C, Carmeliet P, Moermans K, Stockmans I, Smets N, Collen D, Bouillon R, Carmeliet G. Impaired angiogenesis and endochondral bone formation in mice lacking the vascular endothelial growth factor isoforms VEGF164 and VEGF188. Mech Dev. 2002; 111(1–2):61–73. [PubMed: 11804779]
40. Zelzer E, Mamluk R, Ferrara N, Johnson RS, Schipani E, Olsen BR. VEGFA is necessary for chondrocyte survival during bone development. Development. 2004; 131(9):2161–2171. [PubMed: 15073147]
41. Rankin EB, Rha J, Selak MA, Unger TL, Keith B, Liu Q, Haase VH. Hypoxia-inducible factor 2 regulates hepatic lipid metabolism. Mol Cell Biol. 2009; 29(16):4527–4538. [PubMed: 19528226]
42. Storm EE, Kingsley DM. Joint patterning defects caused by single and double mutations in members of the bone morphogenetic protein (BMP) family. Development. 1996; 122(12):3969–3979. [PubMed: 9012517]
43. Merino R, Macias D, Ganan Y, Economides AN, Wang X, Wu Q, Stahl N, Sampath KT, Varona P, Hurle JM. Expression and function of Gdf-5 during digit skeletogenesis in the embryonic chick leg bud. Dev Biol. 1999; 206(1):33–45. [PubMed: 9918693]
44. Wang Y, Wan C, Deng L, Liu X, Cao X, Gilbert SR, Bouxsein ML, Faugere MC, Guldberg RE, Gerstenfeld LC, Haase VH, Johnson RS, Schipani E, Clemens TL. The hypoxia-inducible factor alpha pathway couples angiogenesis to osteogenesis during skeletal development. J Clin Invest. 2007; 117(6):1616–1626. [PubMed: 17549257]
45. Rodda SJ, McMahon AP. Distinct roles for Hedgehog and canonical Wnt signaling in specification, differentiation and maintenance of osteoblast progenitors. Development. 2006; 133(16):3231–3244. [PubMed: 16854976]

46. Kobayashi T, Lu J, Cobb BS, Rodda SJ, McMahon AP, Schipani E, Merkenschlager M, Kronenberg HM. Dicer-dependent pathways regulate chondrocyte proliferation and differentiation. Proc Natl Acad Sci U S A. 2008; 105(6):1949–1954. [PubMed: 18238902]

47. Eshkar-Oren I, Viukov SV, Salameh S, Krief S, Oh CD, Akiyama H, Gerber HP, Ferrara N, Zelzer E. The forming limb skeleton serves as a signaling center for limb vasculature patterning via regulation of Vegf. Development. 2009; 136(8):1263–1272. [PubMed: 19261698]

48. Young AP, Kaelin WG Jr. Senescence triggered by the loss of the VHL tumor suppressor. Cell Cycle. 2008; 7(12):1709–1712. [PubMed: 18583945]

49. Jung YS, Lee SJ, Lee SH, Chung JY, Jung YJ, Hwang SH, Ha NC, Park BJ. Loss of VHL promotes progerin expression, leading to impaired p14/ARF function and suppression of p53 activity. Cell Cycle. 2013; 12(14):2277–2290. [PubMed: 24067370]

50. Cameron TL, Bell KM, Tatarczuch L, Mackie EJ, Rajpar MH, McDermott BT, Boot-Handford RP, Bateman JF. Transcriptional profiling of chondrodysplasia growth plate cartilage reveals adaptive ER-stress networks that allow survival but disrupt hypertrophy. PLoS One. 2011; 6(9):e24600. [PubMed: 21935428]

51. Essers PB, Klasson TD, Pereboom TC, Mans DA, Nicastro M, Boldt K, Giles RH, Macinnes AW. The von Hippel-Lindau tumor suppressor regulates programmed cell death 5-mediated degradation of Mdm2. Oncogene. 2014

52. Zaman F, Menendez-Benito V, Eriksson E, Chagin AS, Takigawa M, Fadeel B, Dantuma NP, Chrysis D, Savendahl L. Proteasome inhibition upregulates p53 and apoptosis-inducing factor in chondrocytes causing severe growth retardation in mice. Cancer Res. 2007; 67(20):10078–10086. [PubMed: 17942942]

53. Malhotra JD, Kaufman RJ. The endoplasmic reticulum and the unfolded protein response. Semin Cell Dev Biol. 2007; 18(6):716–731. [PubMed: 18023214]

54. Tsang KY, Chan D, Bateman JF, Cheah KS. In vivo cellular adaptation to ER stress: survival strategies with double-edged consequences. J Cell Sci. 2010; 123(Pt 13):2145–2154. [PubMed: 20554893]

55. Yeung Tsang K, Wa Tsang S, Chan D, Cheah KS. The chondrocytic journey in endochondral bone growth and skeletal dysplasia. Birth Defects Res C Embryo Today. 2014; 102(1):52–73. [PubMed: 24677723]

56. Schoenfeld AR, Davidowitz EJ, Burk RD. Endoplasmic reticulum/cytosolic localization of von Hippel-Lindau gene products is mediated by a 64-amino acid region. Int J Cancer. 2001; 91(4): 457–467. [PubMed: 11251966]

57. Lai E, Teodoro T, Volchuk A. Endoplasmic reticulum stress: signaling the unfolded protein response. Physiology (Bethesda). 2007; 22:193–201. [PubMed: 17557940]

58. Young AP, Schlisio S, Minamishima YA, Zhang Q, Li L, Grisanzio C, Signoretti S, Kaelin WG Jr. VHL loss actuates a HIF-independent senescence programme mediated by Rb and p400. Nat Cell Biol. 2008; 10(3):361–369. [PubMed: 18297059]

59. Mack FA, Rathmell WK, Arsham AM, Gnarra J, Keith B, Simon MC. Loss of pVHL is sufficient to cause HIF dysregulation in primary cells but does not promote tumor growth. Cancer Cell. 2003; 3(1):75–88. [PubMed: 12559177]

60. Mack FA, Patel JH, Biju MP, Haase VH, Simon MC. Decreased growth of Vhl−/− fibrosarcomas is associated with elevated levels of cyclin kinase inhibitors p21 and p27. Mol Cell Biol. 2005; 25(11):4565–4578. [PubMed: 15899860]

61. Maes C, Goossens S, Bartunkova S, Drogat B, Coenegrachts L, Stockmans I, Moermans K, Nyabi O, Haigh K, Naessens M, Haenebalcke L, Tuckermann JP, Tjwa M, Carmeliet P, Mandic V, David JP, Behrens A, Nagy A, Carmeliet G, Haigh JJ. Increased skeletal VEGF enhances beta-catenin activity and results in excessively ossified bones. Embo J. 2010; 29(2):424–441. [PubMed: 20010698]

62. Puri S, Akiyama H, Hebrok M. VHL-mediated disruption of Sox9 activity compromises beta-cell identity and results in diabetes mellitus. Genes Dev. 2013; 27(23):2563–2575. [PubMed: 24298056]

63. Hattori T, Muller C, Gebhard S, Bauer E, Pausch F, Schlund B, Bosl MR, Hess A, Surmann-Schmitt C, von der Mark H, de Crombrugghe B, von der Mark K. SOX9 is a major negative

regulator of cartilage vascularization, bone marrow formation and endochondral ossification. Development. 2010; 137(6):901–911. [PubMed: 20179096]

64. Kim Y, Murao H, Yamamoto K, Deng JM, Behringer RR, Nakamura T, Akiyama H. Generation of transgenic mice for conditional overexpression of Sox9. J Bone Miner Metab. 2011; 29(1):123–129. [PubMed: 20676705]

Highlights

- VHL is a key regulator of endochondral bone development and bone morphogenesis.
- Loss of VHL does not alter the transition from mesenchymal cells into chondrocytes.
- Loss of VHL impairs chondrocyte proliferation and delays hypertrophy.
- Loss of VHL results in bone deformities in selective sites.
- Loss of VHL causes chondrocyte death in postnatal growth plates.

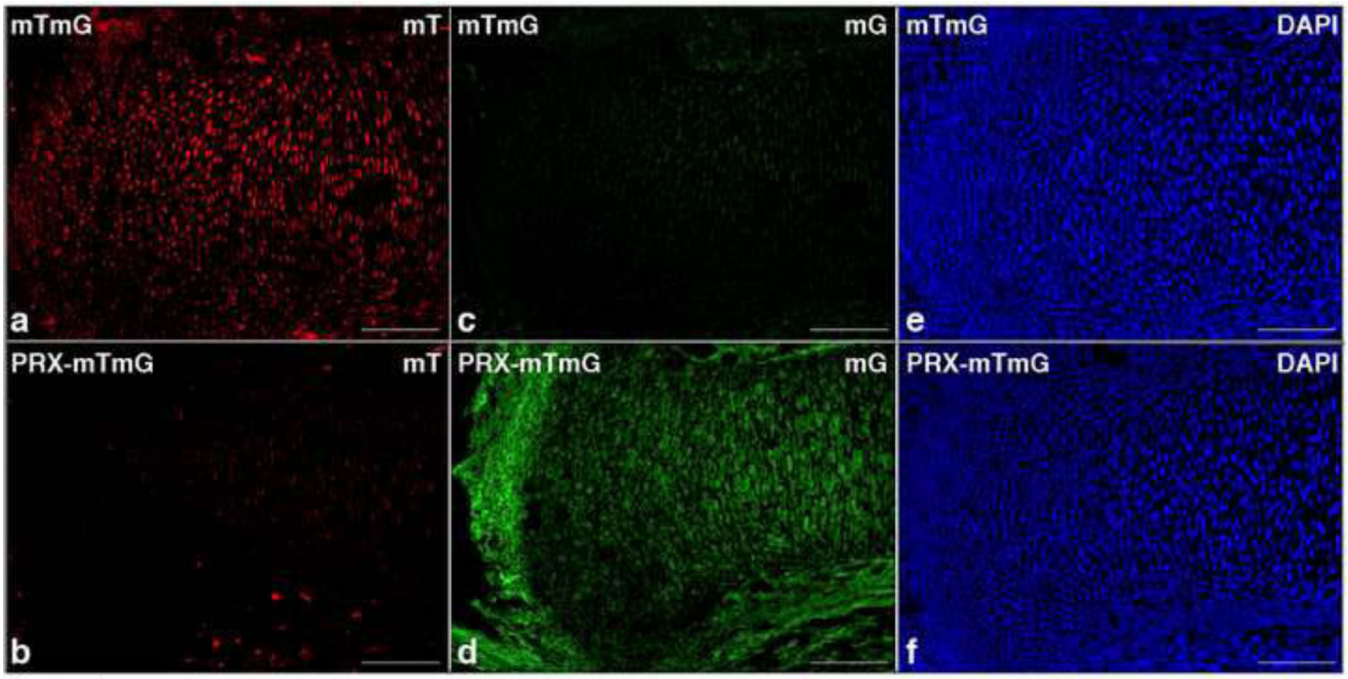

Figure 1. PRX1-Cre expression in fetal growth plate

a-f. Detection of fluorescence in frozen sections of tibias isolated from E15.5 mTmG (upper panels) and PRX-Cre-mTmG (lower panels) mice, respectively. The following abbreviations are used: mT, Membrane-targeted tandem dimer Tomato (a and b); mG, Membrane-targeted EGFP (c and d); DAPI, 4’,6-diamidino-2-phenylindole counterstain (blue nuclei) (e and f). (Bar=250μm).

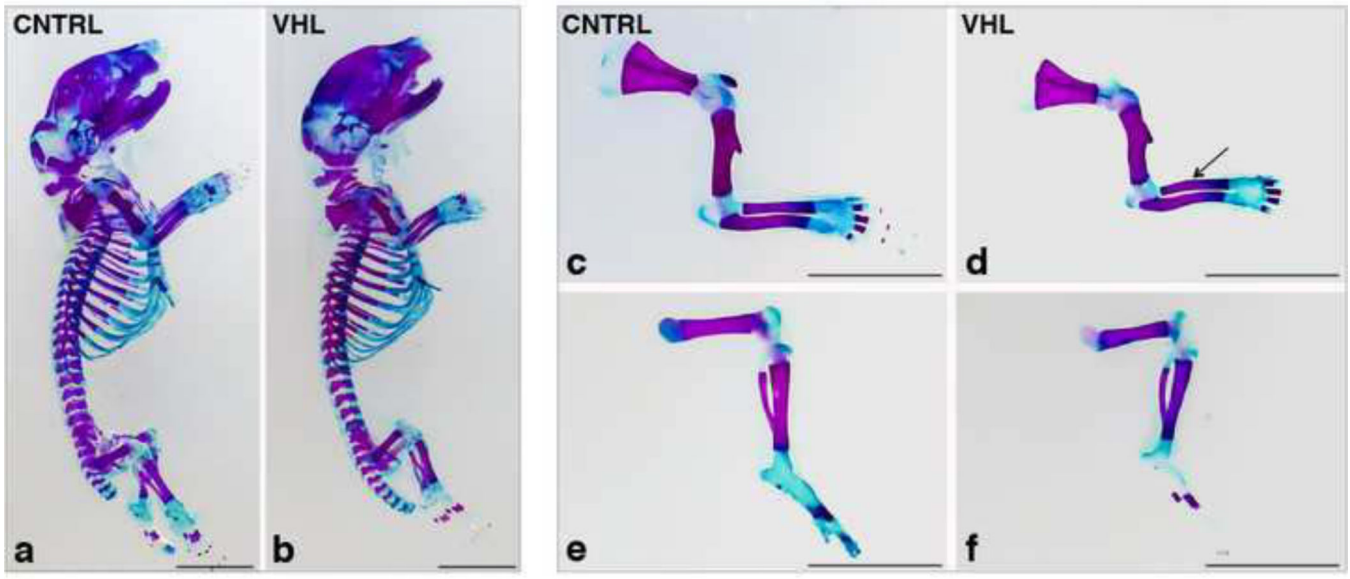

Figure 2. Macroscopic appearance of VHL mice at birth

a,b. Whole mount Alizarin Red S/Alcian blue staining of CNTRL (a) and VHL (b) newborns mice. (Bar=50 mm).

c-f. Whole mount Alizarin Red S/Alcian blue staining of forelimbs (upper panels) and hindlimbs (lower panels) of CNTRL (c and e) and VHL (d and f) mice. The arrow in (d) points at the radius deformity. (Bar=50 mm).

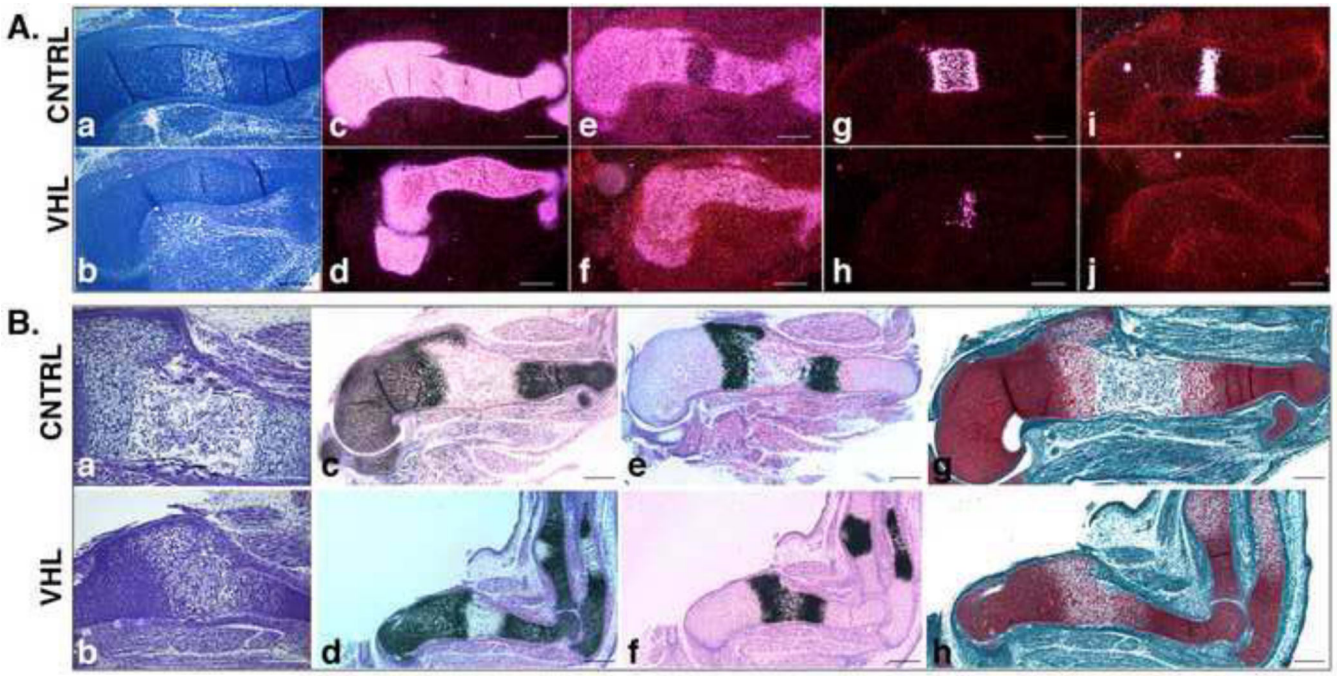

Figure 3. Prenatal growth plate phenotype in VHL mice

A. Delayed terminal differentiation. a,b. H&E staining of E13.5 humerus from CNTRL (a) and VHL (b) specimens. (Bar=250μm).

c-j. *In situ* hybridization for detection of Col2a1 (c and d), Sox9 (e and f), Col10a1 (g and h) and SPP1 (i and j) mRNAs in E13.5 CNTRL (upper row) and VHL (lower row) specimens. Dark-field images are shown. (Bar=250μm).

B. Delay of bone marrow cavity formation a,b. H&E staining of E15.5 humerus isolated from CNTRL (a) and VHL (b) mice. (Bar=250μm).

c-f. *In situ* hybridization for detection of Col2a1 (c and d) and Col10a1 (e and f) mRNAs in E15.5 CNTRL (upper row) and VHL (lower row) samples. Bright-field images are shown. (Bar=250μm).

g,h. Safranin-O staining of E15.5 humerus isolated from CNTRL (g) and VHL (h) mice. (Bar=250μm).

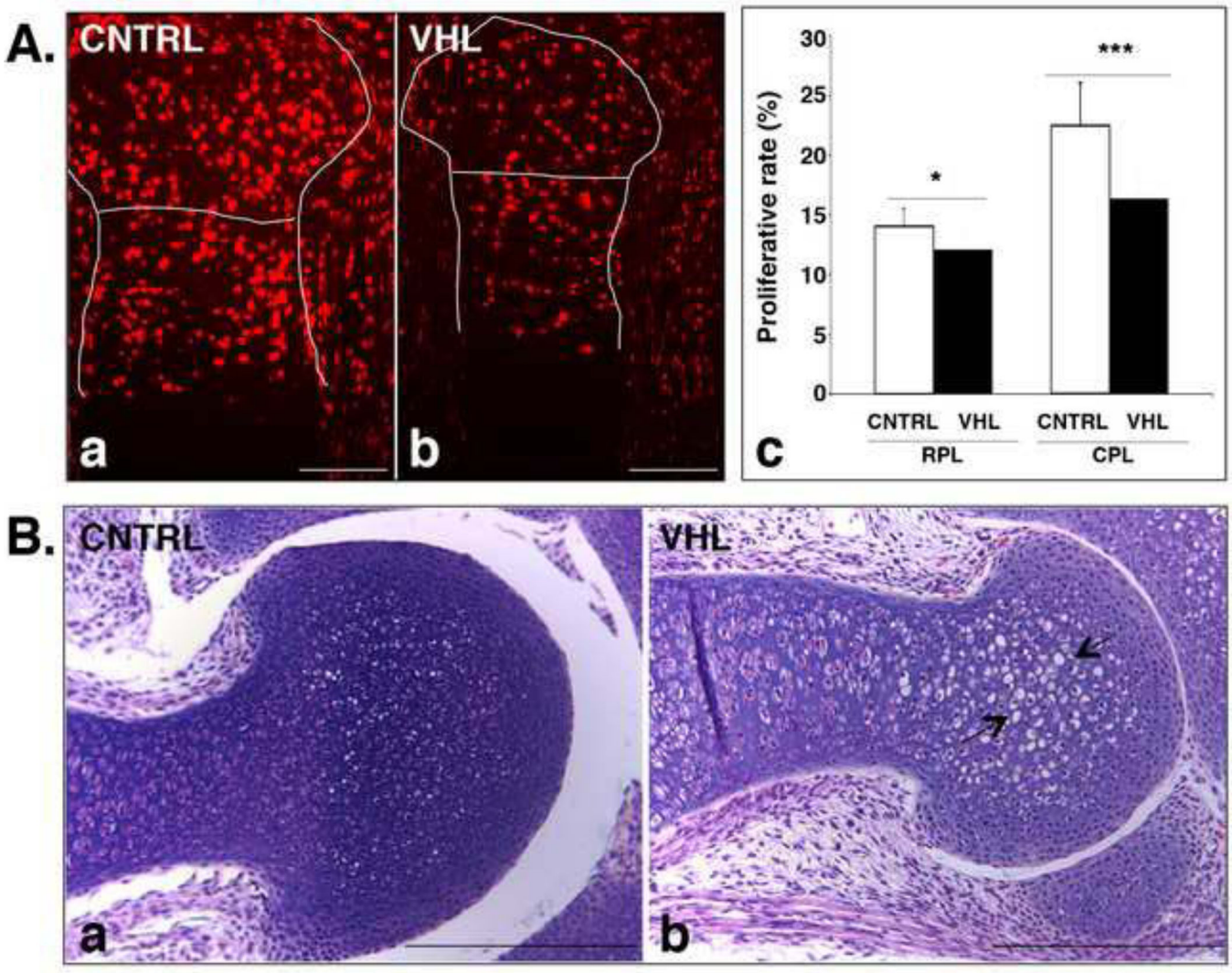

Figure 4. Impaired proliferation and abnormal morphology of VHL chondrocytes

A. Chondrocyte proliferation rate in fetal VHL growth plates. a-c. BrdU assay of E15.5 proximal epiphyses of tibia isolated from CNTRL (a) and VHL (b) mice; quantification of the data is shown in (c) (*: p-value <0.05; ***: p-value <0.001). The lines in (a and b) highlight the growth plate and separate the RPL from the CPL. The following abbreviations are used: RPL, Round Proliferative Layer; CPL, Columnar Proliferative Layer. (Bar=250μm).

B. "Atypical" chondrocytes in absence of VHL. a,b. H&E staining of E17.5 distal humerus in CNTRL (a) and VHL (b) samples. The arrows in (b) point at atypical chondrocytes. (Bar=250μm).

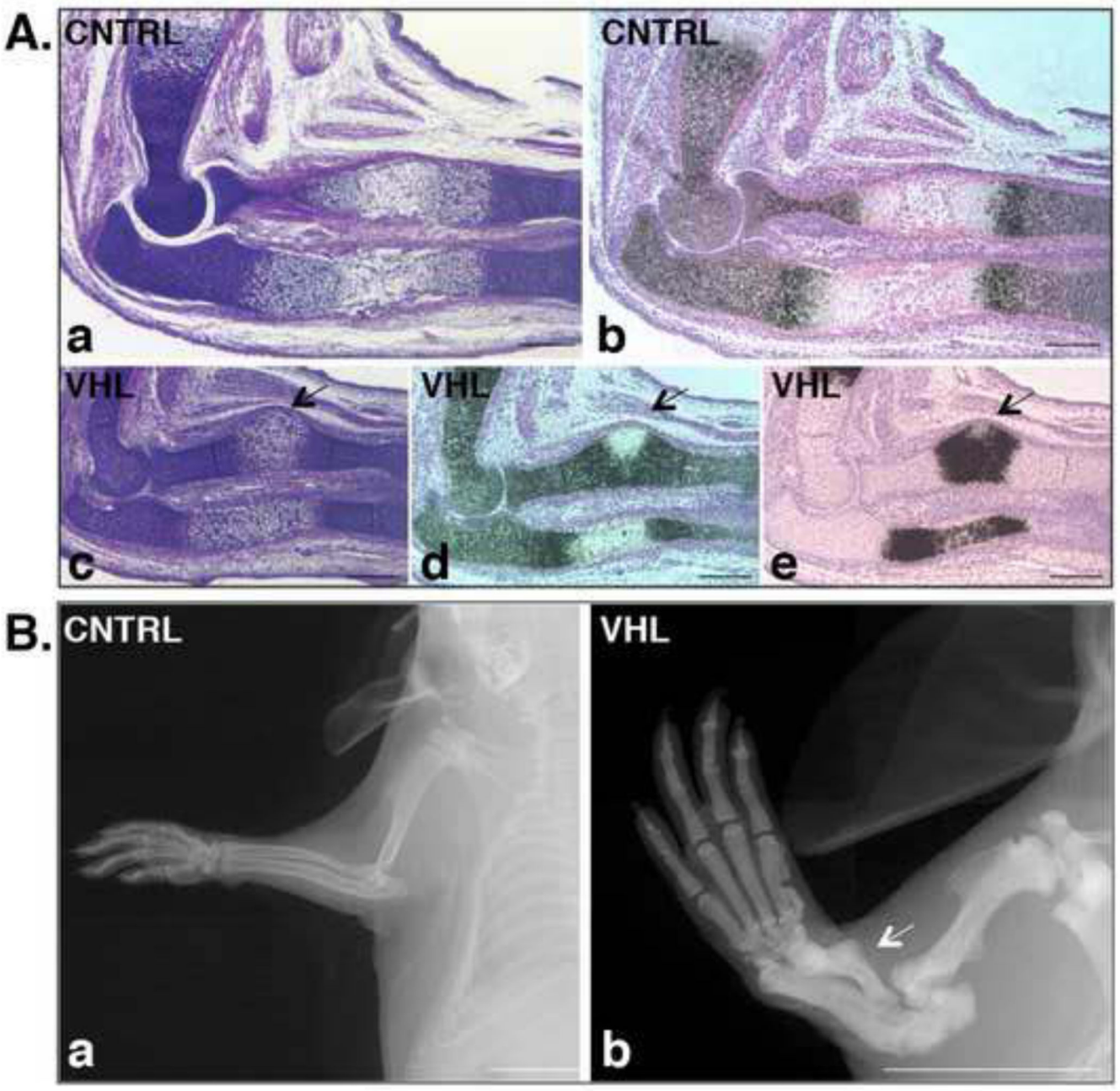

Figure 5. Radius deformity in VHL mice

A. Histological appearance of the radius deformity. a,c. H&E staining of histological sections of E15.5 forelimb isolated from CNTRL (a) and VHL (c) mice. (Bar=250μm). **b,d,e**. *In situ* hybridization for detection of Col2a1 (b and d) and Col10a1 (e) mRNAs in CNTRL (b) and VHL (d and e) specimens. Bright-field pictures are shown. The arrows in (c-e) indicate the deformity of the radius. (Bar=250μm).

B. Postnatal persistence of the radius deformity. a,b. X-rays pictures of p21 forelimb isolated from CNTRL (a) and VHL (b) mice. The arrow in (b) indicates the deformity of the radius. (Bar=1 cm).

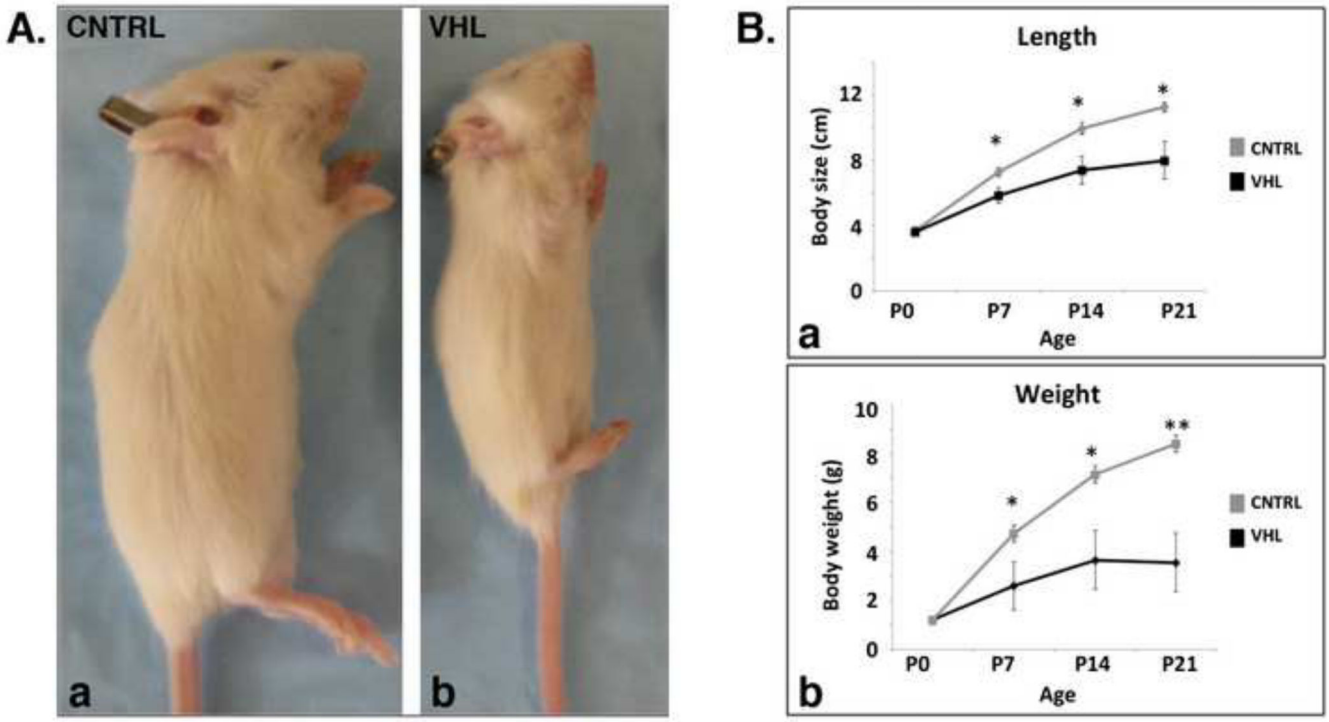

Figure 6. Postnatal growth arrest of VHL mice

A. Macroscopic appearance of VHL mice. a,b. Photograph of p21 CNTRL (a) and VHL (b) mice.

B. Growth curve of VHL mice. a,b, Length (a) and weight (b) curves of CNTRL and VHL mice from p0 to p21. (*: p-value <0.05; **: p-value <0.01).

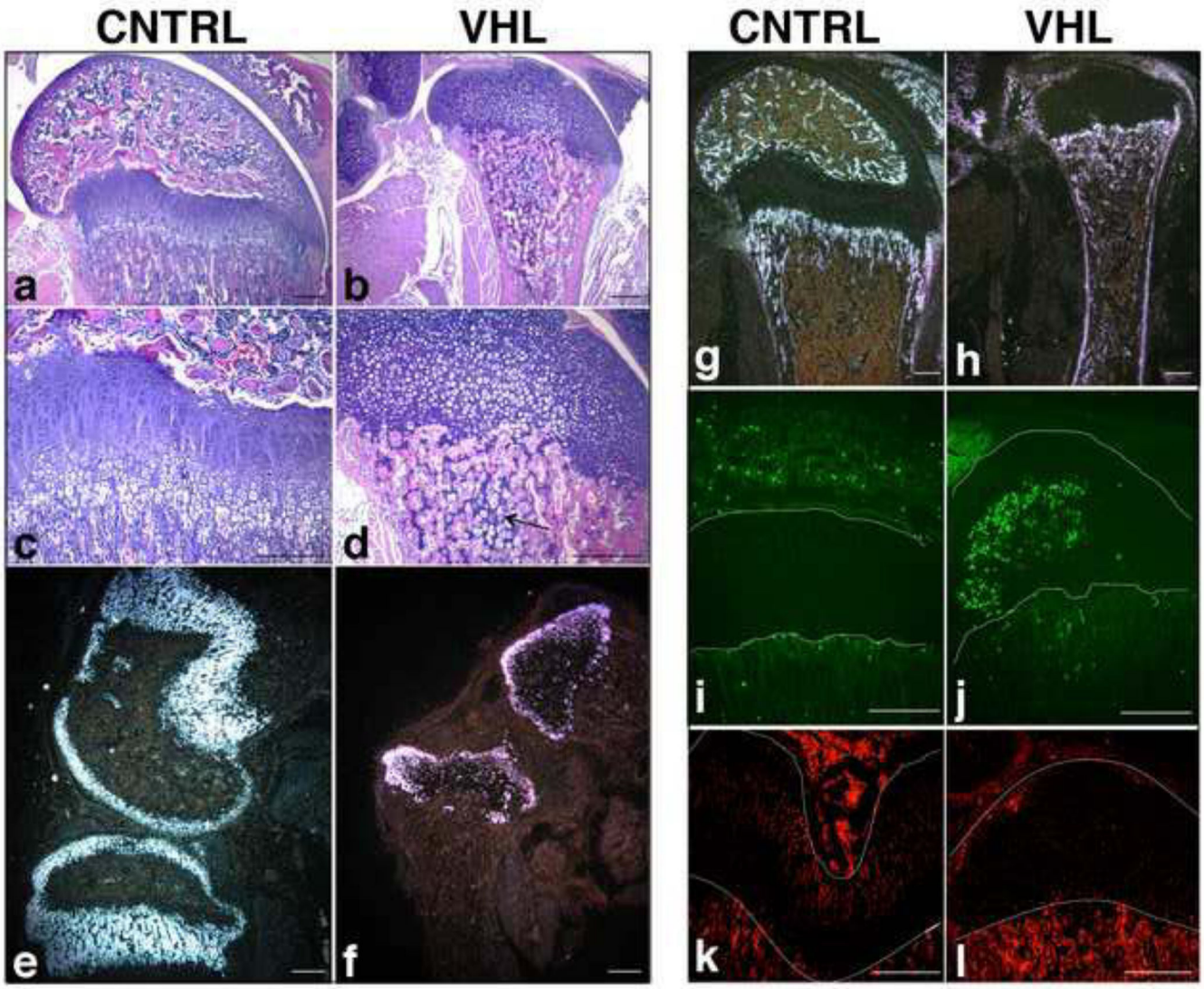

Figure 7. Postnatal growth plate collapse and massive cell death in VHL mice

a-d. H&E staining of p18 distal femur in CNTRL (a) and VHL (b) specimens. Higher respective magnification is shown in panels (c and d). The arrow in (d) indicates the persistence of hypertrophic cartilage within the bone marrow. (Bar=250μm).

e-h. *In situ* hybridization for detection of Col2a1 (e and f) and Col1a1 (g and h) mRNAs in CNTRL (e and g) and in VHL (f and h) p18 distal femur specimens. Dark-fields are shown. (Bar=250μm).

i,j. TUNEL assay in p18 distal femur of CNTRL (i) and VHL (j) specimens. The lines on each panel highlight the growth plate. (Bar=250μm).

k,l. PCNA staining of histological sections of p18 distal epiphyses of femur isolated from CNTRL (k) and VHL (l) mice. The lines on each panel highlight the growth plate. (Bar=250μm).

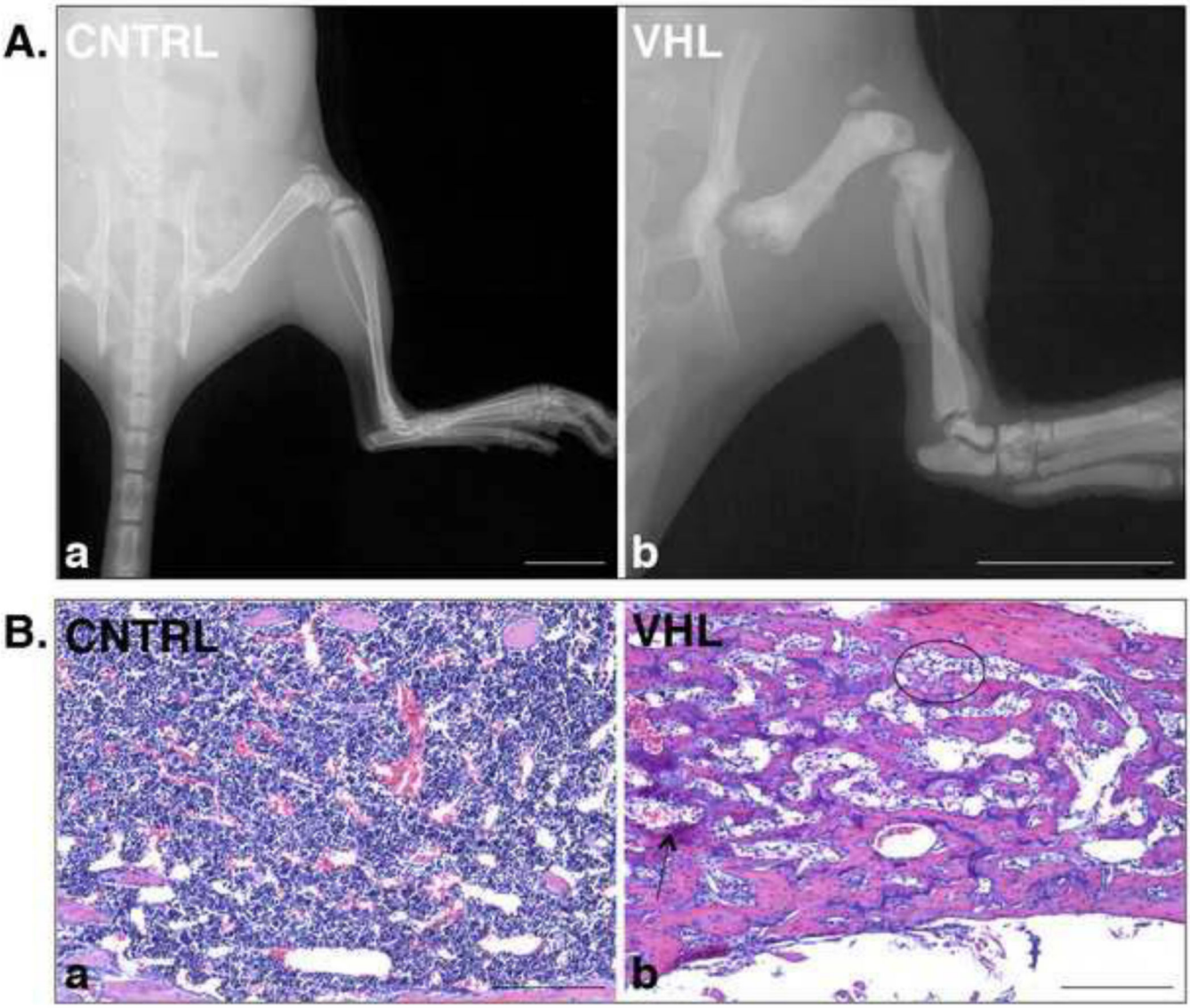

Figure 8. Bone phenotype in VHL mice

A. Radiological appearance of VHL hindlimbs. a,b. X-rays pictures of p21 hindlimb isolated from CNTRL (a) and VHL (b) mice. (Bar=1 cm).

B. Histological appearance of VHL bone. a,b. H&E staining of p17 tibias isolated from CNTRL (a) and VHL (b) mice.

The arrow in (b) points at a dilated blood vessel; the circle in (b) highlights stromal cells in between the bony trabeculae. (Bar=250μm). Please, note the presence of cartilaginous remnants in VHL bone, which could be suggestive of impaired resorption.

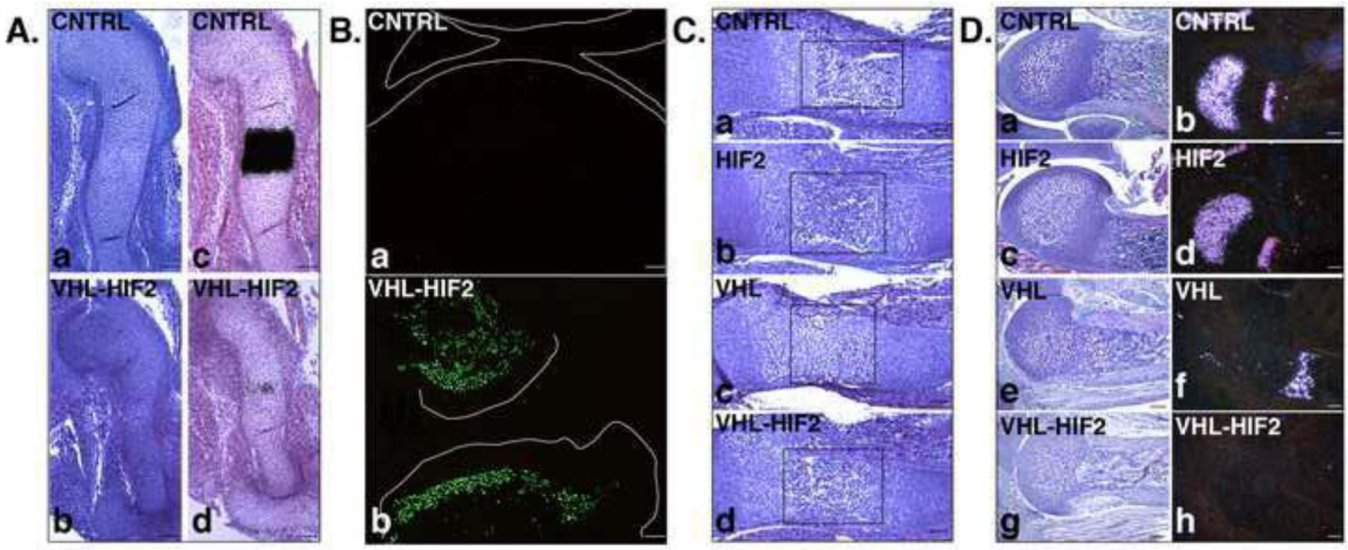

Figure 9. Growth plate phenotype of VHL-HIF2 mice

A. Delayed terminal differentiation. a,b. H&E staining of E13.5 humerus isolated from CNTRL (a) and VHL-HIF2 (b) mice. (Bar=250μm).

c,d. Detection of Col10a1 mRNA by *in situ* hybridization analysis of E13.5 humerus isolated from CNTRL (c) and VHL-HIF2 (d) mice. Bright-field images are shown. (Bar=250μm).

B. Postnatal massive cell death. a,b. TUNEL assay of p21 distal femur and proximal tibia isolated from CNTRL (a) and VHL-HIF2 (b) mice, respectively. The lines on each panel define the joint limits. (Bar=250μm).

C. Partial rescue of bone marrow cavity formation. a-d. H&E staining of E15.5 humerus isolated from CNTRL (a), HIF2 (b), VHL (c) and VHL-HIF2 (d) mice. The rectangles on each panel outline the location of the putative bone marrow cavity. (Bar=250μm). Please, note the very modest delay of terminal differentiation in HIF-2 mice.

D. Premature disappearance of the hypertrophic layer. a,c,e,g. H&E staining of p5 distal growth plate of humerus isolated from CNTRL (a), HIF2 (c), VHL (e) and VHL-HIF2 (g) mice. (Bar=250μm).

b,d,f,h. Detection of Col10a1 mRNA by *in situ* hybridization analysis of p5 distal growth plate of humerus isolated from CNTRL (b), HIF2 (d), VHL (f), VHL-HIF2 (h) mice. Dark-field images are shown. (Bar=250μm).

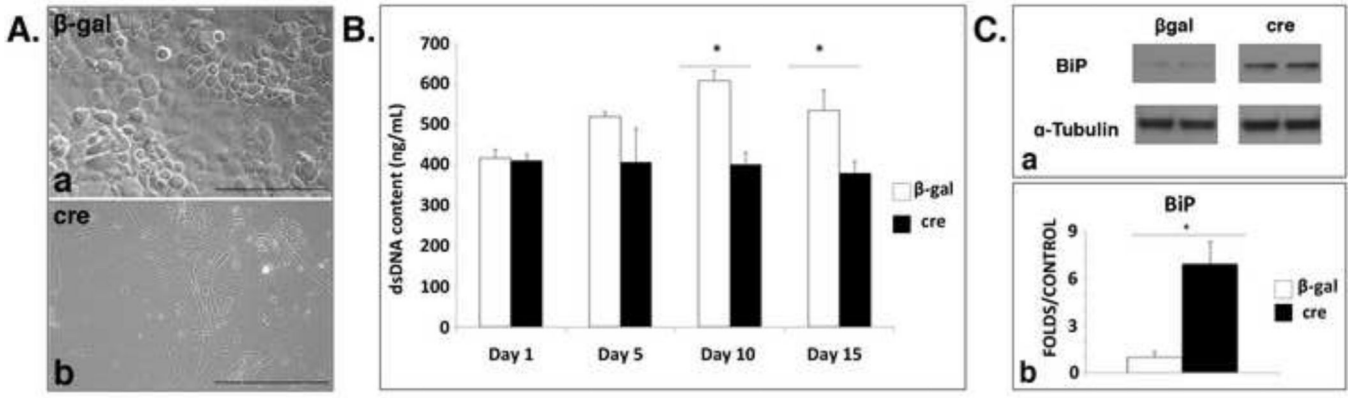

Figure 10. ***In vitro*** **phenotype of chondrocytes lacking VHL**

A. Abnormal morphology of VHL null chondrocytes. a,b. Microscopic pictures of wild type (β-gal) (a) and VHL null (cre) (b) chondrocytes. (Bar=250μm).

B. Growth arrest of VHL null chondrocytes. Picogreen assays in wild type (β-gal) and VHL null (cre) chondrocytes. (*: p-value <0.05).

C. Accumulation of BiP in absence of VHL. a,b. Western blot analysis of BiP in protein lysate from wild type (β-gal) and VHL null (cre) chondrocytes. α-Tubulin was used as a loading control. Quantification of the data is shown in (b) (*: p-value <0.05).